11th U.S. National Combustion Meeting
Organized by the Western States Section of the Combustion Institute
March 24–27, 2019
Pasadena, California

Predicting Cycle-to-cycle Variations in a Spark-ignition Engine using Multi-cycle Large Eddy Simulation

Yunde Su[1], *Derek Splitter*[2], *and Seung Hyun Kim*[1,*]

[1]*Department of Mechanical and Aerospace Engineering, The Ohio State University, Columbus, OH 43210, United States*
[2]*Oak Ridge National Laboratory, 2360 Cherahala Blvd, Knoxville, TN 37932, United States*
[*]*Corresponding author:* kim.5061@osu.edu

Abstract: Multi-cycle large eddy simulation (LES) of a spark-ignition engine has been performed to predict cycle-to-cycle variations (CCV). To describe spark-ignited premixed flame propagation, the front propagation formulation (FPF) method is combined with a laminar-to-turbulent flame transition model that describes the non-equilibrium flame development processes during the initial stage of the kernel growth. In the laminar-to-turbulent flame transition model, the effects of turbulence on the variations in the laminar-to-turbulent flame transition time are modeled based on the Kolmogorov energy cascade. 15 consecutive cycle LES of in-cylinder processes in a spark-ignition four-valve single cylinder engine is conducted. The predicted in-cylinder pressure is compared with the experimental measurements. The range of CCV observed in the experiment is reproduced to an acceptable degree. The predicted CCV is found to be closely related to the difference in the turbulence field near the spark plug around the time of spark discharging, which is consistent with the previous LES studies. The current results also suggest the importance of capturing the variations of the laminar-to-turbulent flame transition in predicting CCV.
Keywords: Large eddy simulation, Cycle-to-cycle variation, Internal combustion engine, Front propagation formulation method

1. Introduction

The combustion process in spark-ignition (SI) engines is typically characterized with some level of cycle-to-cycle variation (CCV). CCV can have a negative effect on vehicle drivability, pollutant emissions and fuel consumption. Understanding, predicting and controlling CCV is thus important for designing SI engines.

3D computational fluid dynamics (CFD) simulation of the flow and combustion processes within SI engines has become an effective approach to study CCV over the past decades. Reynolds Averaged Navier-Stokes (RANS) simulation is widely used in the industry to study the reactive flows in SI engines [1]. However, due to the inherent limitation of ensemble average formulation, RANS is not likely to capture instantaneous fluctuations of local flow, making the prediction of CCV difficult [2]. In contrast, the large eddy simulation (LES) represents a promising approach to study CCV. LES explicitly resolves the large scale turbulent motion and can thus potentially capture the unsteady phenomena contributing to CCV.

The combustion models that have been used in LES of turbulent combustion in SI engines include the extended coherent flamelet model [2, 3], the thickened flame model [4], and the G-equation approach [5]. Kim [6] recently proposed the front propagation formulation (FPF) method

for simulating under-resolved reaction fronts. The FPF method can simulate the flame propagation on the under-resolved grids while retaining the flame structure. In this work, the FPF method is extended to LES of SI engines and used to study the CCV.

In the aforementioned turbulent combustion models, either the sub-filter turbulent flame speed, the filtered flame surface density, or the wrinkling factor needs to be modeled. Theses three terms are actually connected with each other [4, 7]. They are generally modeled with the algebraic formulation [8–10] or the transport equation [2, 3]. The algebraic model is simple in implementation but currently-used models are not able to capture the so-called laminar-to-turbulent flame transition process [11] after spark-ignition [3]. This transition process is found to play an important role in CCV in the recent experimental study by Schiffmann et al. [11] and Zeng et al. [12]. Therefore, the laminar-to-turbulent flame transition deserves to be carefully modeled when an algebraic model is used for flame speed, flame surface density or flame wrinkling factor. In this work, a laminar-to-turbulent flame transition model is proposed and combined with the FPF method. The combined modeling framework is then used to predict the CCV in an experimentally studied SI engine. The effect of the laminar-to-turbulent flame transition model on CCV are also investigated.

2. Turbulent combustion model

The present modeling approach contains three sub-models: the FPF-LES combustion model, the spark-ignition model, and the laminar-to-turbulent flame transition model. The FPF-LES combustion model and the spark-ignition model are used to simulate the under-resolved turbulent flame propagation and the spark ignition, respectively. The laminar-to-turbulent flame transition model is proposed to predict the non-equilibrium transition process after spark ignition.

2.1 FPF-LES combustion model

In premixed combustion simulation, the thermo-chemical state of the mixture can be described by the progress variable c, which is 0 in the unburned mixture and 1 in the burned one. The filtered balance equation for the progress variable can be written as,

$$\frac{\partial \bar{\rho}\tilde{c}}{\partial t}+\frac{\partial \bar{\rho}\tilde{u_j}\tilde{c}}{\partial x_j}=\frac{\partial \bar{\rho}D_t}{\partial x_j}\left(\frac{\partial \tilde{c}}{\partial x_j}\right)+\overline{\omega}_c. \tag{1}$$

In the FPF method, The filtered reaction source term, $\overline{\omega}_c$, in Eq. 1 is expressed as,

$$\overline{\omega}_c=\rho_u S_T|\nabla\psi|, \tag{2}$$

where ρ_u is the unburned density, S_T is the sub-filter turbulent flame speed and ψ is the front structure function. $|\nabla\psi|$ is a discrete regularized Delta function which preserves the sub-filter flame burning rate on an LES grid. ψ is given as,

$$\psi=(1-a)\tilde{c}+a\tilde{c}^{\gamma}, \tag{3}$$

where a and γ are two model parameters satisfying $0\leq a\leq 1$ and $\gamma>1$. In the current work, a is chosen to be 1 and $\gamma=2.5$.

2.2 Spark-ignition model

The combustion is initialized by the spark discharge in SI engines. The initially deposited flame kernel size is typically under-resolved on the LES grid. To capture the under-resolved kernel development, a spark-ignition model adapted from Richard et al. [3] is used here.

The deposited progress variable due to spark discharge can be expressed as,

$$\bar{c}_{spk} = c_0 \exp\left[-\frac{|\mathbf{x}-\mathbf{x}_{spk}|^2}{(0.6\Delta_f)^2}\right], \tag{4}$$

where $\mathbf{x}_{spk}$ is the location of the spark plug and Δ_f is the characteristic scale, which is set to be close to the filter size near the spark plug in this work. c_0 can be determined to match the total deposited mass.

$\bar{c}_{spk}$ can be deposited through the source term in Eq. 1 as,

$$\overline{\omega}_c = \frac{\rho_b \bar{c}_{spk} - \bar{\rho}\tilde{c}}{t_{spk}}, \tag{5}$$

where t_{spk} is the spark characteristic time and can be simply set as the time step in LES. After the initial deposition, the reaction source term for the progress variable is modeled as,

$$\overline{\omega}_c = \rho_u \alpha \tilde{c}(1-\tilde{c}), \tag{6}$$

where α is calculated as,

$$\alpha = \frac{4\pi r_f^2 \langle S_T \rangle_s}{\int \tilde{c}(1-\tilde{c})dv}. \tag{7}$$

$\langle\cdot\rangle_s$ denotes flame surface averaging. The spark ignition model is used until the maximum progress variable, $\tilde{c}_{max}$, reaches one. After that, the progress variable source term is modeled with the FPF method, i.e. Eq. 2.

2.3 Laminar-to-turbulent flame transition model

The flame wrinkling during the early kernel development is highly non-equilibrium and transitional [3]. To capture this transition process, it is assumed that the sub-filter flame speed S_T in Eqs. 2 and 7 gradually increases from the laminar flame speed, S_L, to the equilibrium state turbulent flame speed, S_T^{eq}. S_T^{eq} can be calculated with an algebraic model, e.g. the LES version [5] of Peters flame speed model [13]. This laminar-to-turbulent flame transition process is thus modeled as,

$$S_T = (1-w)S_L + wS_T^{eq}, \tag{8}$$

where w is the weight controlling the transition from the laminar flame speed to the equilibrium turbulent flame speed. w is modeled as,

$$w = \frac{1}{2}\left\{\tanh\left[\frac{4(r_f-\eta_i)}{\eta_o-\eta_i} - 2\right] + 1\right\}, \tag{9}$$

where r_f is the mean flame kernel radius. η_i represents the flame radius where the laminar-turbulent flame transition starts and η_o the flame radius where the kernel becomes fully turbulent. η_i and η_o are therefore called the inner transition scale and the outer transition scale, respectively.

Bore(mm)	86	Speed(r/min)	2006
Stroke(mm)	86	Spark timing (°CA)	-2.2
Compression ratio	9.0	Intake valve timing(°CA)	IVO=307,IVC=571
Fuel-air ratio	1.0	Exhaust valve timing(°CA)	EVO=137,EVC=375
Fuel	Isooctane		

Table 1: Engine specifications.

It is noted that the laminar-to-turbulent flame transition process can have significant variations from cycle to cycle, which plays an important role in CCV [11, 12]. These variations are closely related to the flame-turbulence interaction. The more energetic is turbulence, the sooner will the kernel transit from the laminar to the turbulent flame. The variations in the transition can be captured through suitable models for η_i and η_o in Eq. (9).

The inner scale, η_i, is expected to be less sensitive to this flame-turbulence interaction and can thus be approximated as a constant on the order of the laminar flame thickness, l_F. Variations in the outer transition scale, η_o, due to varying turbulence intensity is expected to account for the major portion of variations in the laminar-to-turbulent flame transition. The Gibson scale represents the size of the smallest eddies that can wrinkle a flame [14]. It can thus be hypothesized that a flame becomes fully turbulent when the size of the flame kernel becomes much larger than the Gibson scale. This leads to

$$\eta_o = k l_G, \tag{10}$$

where k is a model constant larger than 1. l_G can be estimated based on the Kolmogorov cascade theory:

$$l_G = \overline{\left(\frac{\Delta}{(u'_\Delta)^3}\right)} S_L^3, \tag{11}$$

where u'_Δ and Δ represent sub-filter turbulence intensity and the filter size, respectively. The overline in Eq. 11 denotes an averaging operation. Averaging is taken near the spark-plug at the time of spark discharge. The combination of Eq. 10 and Eq. 11 indicates that the outer transition scale η_o scales with the ratio of S_L to u'_Δ. This correlation is consistent with the above discussion on the laminar-to-turbulent flame transition.

3. Multi-cycle LES of SI engine

3.1 Engine configuration and case set-up

The engine under consideration is a single-cylinder version of the GM LNF 2.0L 4-cylinder design turbocharged gasoline direct injection (GDI) engine from the 2007 Pontiac Solstice. In the current simulation, sprays are not considered and the gaseous premixed fuel/air mixture is assumed to enter into the cylinder through the intake port. The engine configuration is shown in Fig. 1. The main characteristics of the experimental setup are summarized in Tab. 1.

The multi-cycle LES was performed using the commercial CFD code CONVERGE v2.3.Multiple cycles were simulated consecutively without having any treatment between the cycles. The pro-

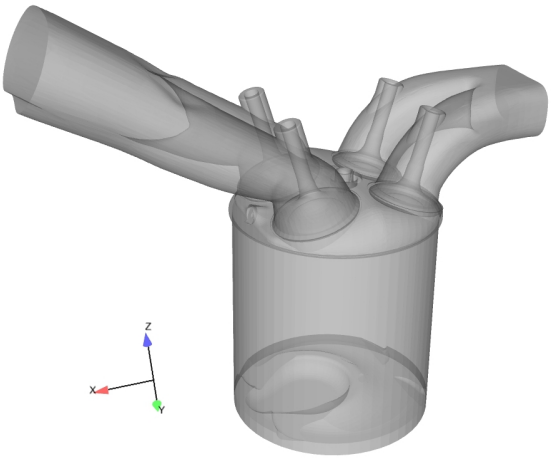

Figure 1: Engine configuration.

posed combustion models are implemented into CONVERGE with user defined functions. The one-equation dynamic structure model [15] is used to simulate the turbulent sub-grid stresses.

The cut-cell Cartesian mesh approach is used in CONVERGE to discretize the computational domain. The adaptive mesh refinement (AMR) strategy based on velocity gradient is employed. The mesh is refined near the spark-plug around the ignition timing and the flame front. The total number of computational cells during the simulation ranges from 1.8M to 18M. The simulation is performed on the Owens system in the Ohio Supercomputing Center. 140 cores are used from -130°CA to 370°CA while 280 cores are used from 370°CA to 590°CA. The computation of a full cycle takes about 56 hours.

3.2 Simulation results and discussion

The simulation of fifteen consecutive cycles has been performed. The predicted in-cylinder pressure is shown in Fig. 2 with comparison to the experimental data. Overall, CCV in the simulation is comparable to that in the experiment. It is also noted that the simulation results show a consistently higher peak pressure compared with the experimental data, similar to the engine LES result with CONVERGE in Zhao et al. [10]. This is possibly due to that the flame-wall interaction is currently not modeled.

To compare LES results with experiment data more rigorously, the coefficient of variance (COV) of the maximum pressure and burn rate-related parameters (CA10, CA50 and CA10-75) are calculated. The result is shown in Fig. 3. COVs in the experiment are evaluated for 5000 cycles, in contrast to 15 cycles in LES. The COVs in the simulation is close to those in the experiment with the largest difference to be 3.73% and the smallest difference to be 0.06%. Table 2 shows the comparison of the standard deviation (SD) for CA10, CA50, and CA10-75. The comparison is similar to that for COV in Fig. 3.

Fig. 4 shows the flame front evolution in the fast cycle, defined as the cycle with the highest peak pressure, and in the slow cycle, defined as the cycle with the lowest peak pressure. The flame burns much faster in the fast cycle, resulting in much higher pressure rise as shown in Fig. 2. Fig. 5 shows the comparison of the sub-grid turbulent kinetic energy at 0°CA between the fast cycle and

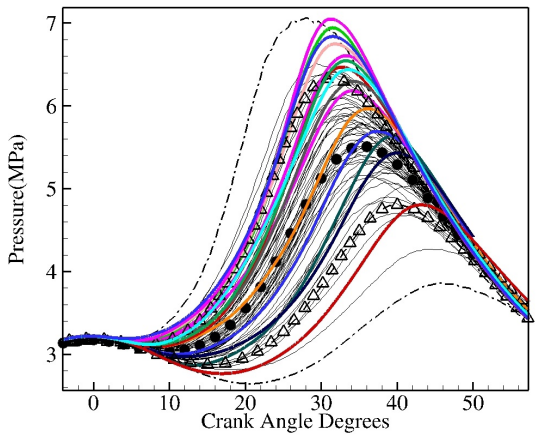

Figure 2: Predicted in-cylinder pressure in multi-cycle LES using the FPF method (black thin lines: 50 cycles from the experiment, colored thick lines: 15 LES cycles, dashed-dotted lines: fastest and slowest cycles in the experiment, triangle: 5% and 95% bounds from 5000 cycles in experiment, circles: measured mean pressure in experiment).

	CA10	CA50	CA10-75
LES	2.4	3.2	1.3
Experiment	1.8	2.6	1.4

Table 2: Comparison of the predicted SDs for CA10, CA50, and CA10-75 with the experiment data.

the slow cycle. It is evident that the sub-grid turbulent kinetic energy near the spark-plug in the fast cycle is higher than that in the slow cycle. The observed dependence of CCV on the turbulence field is consistent with the previous studies [2, 16].

Table 3 compares the laminar-to-turbulent flame transition parameters between the fast cycle and the slow cycle. The flame speed is similar while the turbulence intensity is much higher in the fast cycle. As a result, the transition outer scale η_o is smaller, resulting in faster flame development as shown in Fig. 4. Without the variation in the flame transition model, the difference between the fast cycle and the slow cycle would be much smaller.

Variations in the mixture composition are neglected in the current work by assuming the mix-

	$\overline{\left(\frac{(u'_\Delta)^3}{\Delta}\right)}(m^2/s^3)$	$\overline{u'_\Delta}(m/s)$	$\overline{S_L}(m/s)$	$\eta_o(mm)$
Fast cycle	5.65×10^3	0.82	0.71	1.23
Slow cycle	1.52×10^3	0.25	0.71	4.76

Table 3: Comparison of laminar-to-turbulent flame transition model parameters in the fast cycle with those in the slow cycle.

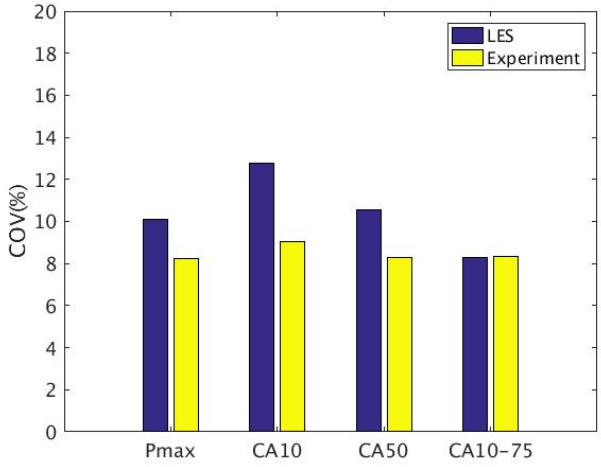

Figure 3: Comparison of the predicted COVs for the maximum pressure, CA10, CA50, and CA10-75 with the experiment data.

ture to be fully premixed. While some previous studies have shown that the effects of mixture composition variations on CCV are much less significant compared with those of variations in in-cylinder flow [10], future work should be directed to investigate the effects of direct injection and associated mixture stratification in the GDI engine.

4. Conclusion

The CCV of an experimental four-valve single cylinder SI engine is studied with a newly developed LES combustion modeling approach. The modeling approach consists of three parts: the FPF method to describe the under-resolved the flame front movement, the spark-ignition model to capture the spark-ignition process, and a laminar-to-turbulent flame transition model to simulate the non-equilibrium flame transition process. The novelty of the proposed model is that it can capture the variations in the laminar-to-turbulent flame transition, which has been found to be important in CCV in experiments.

15 consecutive cycle LES of the SI engine with the proposed modeling approach is conducted to study the CCV. The predicted degree of CCV is comparable to that shown in the experiment. Moreover, the LES results show that the CCV is correlated with the turbulence field near the spark-plug around the spark timing for the current configuration. The difference in the turbulence field causes the variations in the laminar-to-turbulent flame transition, which strongly affects the level of the predicted CCV. This result suggests the importance of capturing the variations in laminar-to-turbulent flame transition in designing combustion models to predict CCV.

5. Acknowledgements

This material is based upon work supported by the Department of Energy, Office of Energy Efficiency and Renewable Energy (EERE) and the Department of Defense, Tank and Automotive Re-

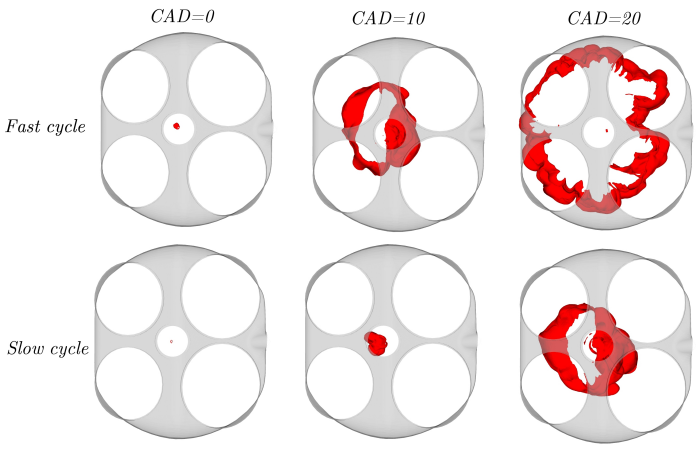

Figure 4: Comparison of flame front evolution between the fast cycle and the slow cycle (the red color denotes the iso-surface of $\tilde{c} = 0.5$; the grey color denotes the engine head).

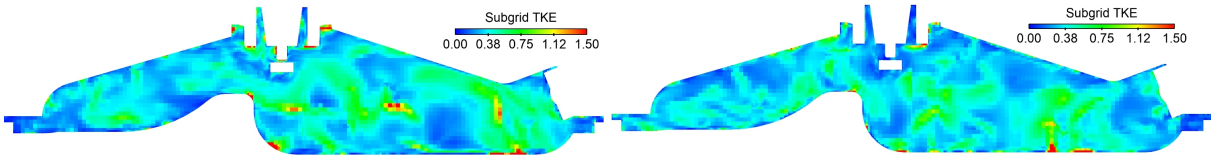

(a) Fast cycle (b) Slow cycle

Figure 5: Comparison of sub-grid turbulent kinetic energy at 0°CA in the fast cycle with that in the slow cycle.

search, Development, and Engineering Center (TARDEC), under Award Number DE-EE0007334. The authors also thank the Ohio Supercomputer Center (OSC) for providing the computational resource.

References

[1] M. Drake and D. Haworth, Advanced gasoline engine development using optical diagnostics and numerical modeling, Proceedings of the Combustion Institute 31 (2007) 99–124.

[2] O. Vermorel, S. Richard, O. Colin, C. Angelberger, A. Benkenida, and D. Veynante, Towards the understanding of cyclic variability in a spark ignited engine using multi-cycle LES, Combustion and Flame 156 (2009) 1525–1541.

[3] S. Richard, O. Colin, O. Vermorel, A. Benkenida, C. Angelberger, and D. Veynante, Towards large eddy simulation of combustion in spark ignition engines, Proceedings of the Combustion Institute 31 (2007) 3059–3066.

[4] O. Colin, F. Ducros, D. Veynante, and T. Poinsot, A thickened flame model for large eddy simulations of turbulent premixed combustion, Physics of fluids 12 (2000) 1843–1863.

[5] H. Pitsch, A consistent level set formulation for large-eddy simulation of premixed turbulent combustion, Combustion and Flame 143 (2005) 587–598.

[6] S. H. Kim, A front propagation formulation for under-resolved reaction fronts, J. Comput. Phys. 285 (2015) 193–207.

[7] D. Veynante and V. Moureau, Analysis of dynamic models for large eddy simulations of turbulent premixed combustion, Combust. Flame 162 (2015) 4622–4642.

[8] V. Granet, O. Vermorel, C. Lacour, B. Enaux, V. Dugué, and T. Poinsot, Large-Eddy Simulation and experimental study of cycle-to-cycle variations of stable and unstable operating points in a spark ignition engine, Combustion and Flame 159 (2012) 1562–1575.

[9] M. Schmitt, R. Hu, Y. M. Wright, P. Soltic, and K. Boulouchos, Multiple cycle LES simulations of a direct injection natural gas engine, Flow, Turbulence and Combustion 95 (2015) 645–668.

[10] L. Zhao, A. A. Moiz, S. Som, N. Fogla, M. Bybee, S. Wahiduzzaman, M. Mirzaeian, F. Millo, and J. Kodavasal, Examining the role of flame topologies and in-cylinder flow fields on cyclic variability in spark-ignited engines using large-eddy simulation, International Journal of Engine Research (2017) 1468087417732447.

[11] P. Schiffmann, D. L. Reuss, and V. Sick, Empirical investigation of spark-ignited flame-initiation cycle-to-cycle variability in a homogeneous charge reciprocating engine, International Journal of Engine Research 19 (2018) 491–508.

[12] W. Zeng, S. Keum, T.-W. Kuo, and V. Sick, Role of large scale flow features on cycle-to-cycle variations of spark-ignited flame-initiation and its transition to turbulent combustion, Proceedings of the Combustion Institute (2018).

[13] N. Peters, The turbulent burning velocity for large-scale and small-scale turbulence, Journal of Fluid mechanics 384 (1999) 107–132.

[14] N. Peters, Turbulent combustion, Cambridge university press, 2000.

[15] E. Pomraning, Development of large eddy simulation turbulence models, PhD thesis, University of Wisconsin–Madison, 2000.

[16] K. Truffin, C. Angelberger, S. Richard, and C. Pera, Using large-eddy simulation and multivariate analysis to understand the sources of combustion cyclic variability in a spark-ignition engine, Combustion and Flame 162 (2015) 4371–4390.